Atomic, surface morphology, structural and electrochemical properties of silver nanoparticles-polypyrrole composite film grown on cellulosic paper substrate

Abderrazak HAMAM (hamam.abderrazak@yahoo.com)
CRTI: Centre de Recherche en Technologies Industrielles https://orcid.org/0000-0003-1817-5506
Mounira Maiza
CRTI: Centre de Recherche en Technologies Industrielles
Mohamed Mehdi Chehimi
Universite de Paris
Dahbia Oukil
Universite de Bejaia

Research Article

Keywords: Paper substrate, Polypyrrole, Silver, Composite materials, Electrode materials

Posted Date: September 29th, 2021

DOI: https://doi.org/10.21203/rs.3.rs-915254/v1

Abstract

In this work, we describe a simple strategy for the preparation of a low-cost electrode material based on polypyrrole (PPy) film grown on an insulating cellulosic paper substrate (Pap) via in-situ oxidative polymerization technique and functionalized by silver nanoparticles (AgNPs) uniformly dispersed on its surface. The properties of the obtained AgNPs-PPy composites were characterized using FTIR-ATR spectroscopy (FTIR-ATR), X-ray photoelectron spectroscopy (XPS), Scanning Electron Microscope (SEM) coupled with energy dispersive X-ray spectrometry (EDX), X-ray diffraction spectroscopy (DRX) and electrochemical impedance spectroscopy (SIE).

Introduction

Today, conductive polymers (CPs) are still the subject of much research both on the fundamental level and on the level of their potential applications. Until now, the major drawback resided in the difficulties of implementation and in their modest mechanical and electrical properties. In order to maximize their use, researchers have concentrated on the production of composite materials by incorporating or depositing these conductive polymers on insulating supports such as textiles, paper, wood and plexiglass (Hamam et al. 2015, Aitout et al. 2006). Indeed, these CPs coated insulating supports and decorated by metal particles have good electrical conductivity, thermal and flexible properties for a number of applications such as flexible and foldable devices (Santhiago et al 2016), energy storage (Tian et al 2017), electronic inks (Jia et al 2014), electrocatalysis (Hamam et al. 2015, Aitout et al. 2006).

On the one hand, polypyrrole (PPy) is the conductive polymer of the material having good electrical conductivity, good stability and easy to synthesize chemically in an aqueous medium. On the other hand, once synthesized, it is in the form of a granular powder, it is not very difficult to obtain a deposit of good mechanical and electrical properties. For the purpose of coating materials, especially non-conductive supports with PPy films, it is desirable to decrease bulk polymerization as much as possible. This can usually be achieved by selecting the reaction conditions and the appropriate treatment of the surface of the material to be covered. Although bulk polymerization is not completely eliminated, a relatively high yield of the polymeric deposits can be achieved by adjusting the reaction conditions as the monomer diffusion time, polymerization time, oxidizing/monomer molar ratio, temperature (Hamam et al. 2015; Aitout et al. 2006). The incorporation of PPy on cellulosic paper supports is an interesting strategy to achieve for obtaining conductive films at low cost and with interesting mechanical properties.

The combination of conducting polymers with metal particles gives a promising way to strengthen the CPs as well as introducing electrical properties based on the electrical synergy between the two components (Ma et al 2015; Kazemi et al 2015).The Incorporation of noble metal nanoparticles into the polymer matrix has been extensively studied to increase the conductivity (ˇSkodovà et al 2013), to enhance the electrochemical strain (Hara et al 2004) of the CPs, to modify the CPs film morphology during preparation process (Liu et al 2006), and on the other hand, using the CPs as support to improve the electrocatalysis of several redox reactions (Oukil et al 2013, Mokrane et al 2008).

The paper-based electrodes described in this work are low cost compared to traditional electrodes materials. In addition, the paper electrode materials are flexible and can be easily cut with scissors. These features have motivated our work towards the development of low-cost electrode materials. The films of polypyrrole decorated with silver nanoparticles have attracted great attention due to applications in several fields such as medical devices (You et al 2012), antimicrobial biomaterials (Maráková et al 2017), electrocatalysis (Lu et al 2012) and electroanalysis (Nia et al 2015 ; Bonacic-Koutecky et al 2012).

Experimental

Reagents

Pyrrole (>98% purity, Prolabo product) is used as received in the chemical synthesis of Polypyrrole. Iron (III) chloride anhydrous ($FeCl_3$) (Prolabo products) were used as the oxidants for the polymerization of polypyrrole. Sulfuric acid (H_2SO_4), Potassium chloride (KCl), Potassium hydroxide (KOH), silver nitrate ($AgNO_3$) was purchased from Merck. All aqueous solutions were prepared with bi-distilled water (presenting high resistance ~18MΩ). This procedure was sufficient to obtain reproducible results. The paper semi rigid substrate used presents a surface density of 240-250 $g.m^{-2}$ (ISO536). The geometric surface of the working electrode was equal to 2 cm^2.

Paper substrate coating process

Aqueous solution of pyrrole, 0.1M of KCl and pH acid medium were employed to carry out the synthesis. The H_2SO_4 acid was employed to neutralize the positive charges created during the synthesis of polypyrrole and it also acted as doping counter ions. The following stage was the adsorption of pyrrole and the doping acid on the fabric. After this time, an oxidizing solution of iron (III) chloride solution was added. The oxidant to monomer ratio was fixed to 2 which was the optimal found in bibliography (Sparavigna et al 2010). Different synthesizing durations in the presence of the oxidant were tested in view to optimize the process (reactivity tests). After being deposited PPy onto paper substrate, the electrode was washed with triply distilled water and subjected to its characterization. The electrochemical characterization by voltammetry and electrochemical impedance spectroscopy (EIS) of a deposited PPy/Pap sheet was performed using the film as the working electrode in 0.1 $mol.L^{-1}$ KOH solution. The reactivity of the obtained electrode was tested and an optimal value of synthesizing durations was fixed. The polymerization experiments were conducted at 0 °C. Scheme 1

Preparation of modified AgNPs-PPy/Pap electrodes

The PPy/Pap electrode (surface of 2 cm^2) is dipped during 5,10 and 15 min, respectively in a solution containing $AgNO_3$, Different amounts of concentration $AgNO_3$ and synthesizing durations were tested in view to optimize the process (reactivity tests). After being deposited Ag nanoparticles onto PPy/Pap film, the electrode is washed with triply distilled water and subjected to its characterization. The electrochemical characterization by cyclic voltammetry and electrochemical impedance spectroscopy

(EIS) of a deposited AgNPs-PPy/Pap sheet was performed using the film as the working electrode in 0.1 mol.L^{-1} KOH solutions. Scheme 1

Apparatus

For electrochemical measurements, the experiments were carried out in a conventional three-electrode double walled cylindrical glass cell. A saturated calomel electrode (SCE) placed in a separate compartment containing the supporting electrolyte and a platinum wire electrode were used as reference and auxiliary electrode, respectively. The polarization curves, at a scan rate of 20 mV.s^{-1}, and electrochemical impedance spectroscopy (EIS) tests were carried out in aerated solution using an AUTOLAB Potentiostat/Galvanostat (SP-150) Biologic SAS under FRA software. For EIS tests, we measured the response of our electrochemical system to alternating current (a.c) excitation with a frequency ranging from 100 kHz to 100 mHz and peak to peak a.c. amplitude of 10 mV. The impedance diagrams are given in the Nyquist representation. Infrared spectra were recorded using a Bruker apparatus operating in ATR mode. The morphology performed by field emission gun-scanning electron microscope (SEM, Carl Zeiss). X-ray photoelectron spectra were recorded using a K Alpha system (Thermo Fisher Scientific, Al X-ray source hv = 1486.6 eV; spot size = 400 µm).

Results And Discussion

Characterization of PPy/Pap and AgNPs-PPy/Pap films

FTIR-ATR spectroscopy

The FT-IR spectra of uncoated paper substrate and PPy coated Pap is shown in Fig. 1 The spectrum (a) Pap shows the typical absorption bands characteristic of cellulose. The band at 3340 $cm^{-1}$is attributed to the stretching vibration O-H bonds of the alcohol functions of cellulose (Sain et al 2006). Absorption bands located around 2924 cm^{-1} and 1160 cm^{-1} are respectively associated to the stretching vibration C–H in cellulose (Kaushik et al 2011) and the stretching vibrations of the C–O–C bond (He et al 2007). The band at 1030 is attributed to the stretching vibration C-O bond (Hu et al 2011).The presence of the C-H group is supported by the vibration band around 1438 cm^{-1} (Ul-Islama et al 2012) and the bands near 1315 cm^{-1} and 1248 cm^{-1} are attributed to O–H deformation bonds.

The PPy/Pap composite displays all of the characteristic bands of the PPy phase (spectrum (b)), indicating the effective formation of PPy by in-situ oxidative polymerization. The peak located at 1540 cm^{-1} is related to C-N/C = C stretching mode of the Pyrrole ring (Yuana et 2016; Feng et al 2007). The peaks at 1300 and 1160 cm^{-1} are assigned to C-H in-plane vibration (Wei et al 2010), and the band at 1450 cm^{-1} are due to C-N stretching of PPy (Patil et al 2013). Moreover, the peaks near 960 and 890 cm^{-1} are caused by the C-H wagging vibration of doped PPy (Das et 2013) and the N-H_2 wagging vibration in the PPy is initiated at 790 cm^{-1} (Wang et al 2004). The characteristic band of the hydroxyl groups of the

cellulose (3340 cm^{-1}) disappeared in the PPy/Pap composite and this disappearance is due to the physicochemical interactions of the OH groups of the cellulosic paper with the polypyrrole matrix to form the conductive composite. Moreover, it is also observed that the absorption bands at 1160 and 1030 cm^{-1} are still present in the composite but with a low intensity and a low chemical shift due to the interactions between the cellulose chains and the polypyrrole cycles (Hu et al 2011). The AgNPs-PPy composite exhibits an FT-IR spectrum similar to PPy with the bands for C–N stretching and C–H plane vibration and N–H stretching but with a low intensity and a low chemical shift. These shifts reflect the interaction of the incorporated silver with the polymer backbone (Zhang et al 2014).

X-ray Photoelectron Spectroscopy

XPS was used to determine the surface elemental and chemical composition of the pristine and modified paper samples. Figure 2 displays typical survey spectra of paper, PPy/Pap and AgNPs-PPy/Pap samples. The main labeled peaks are C1s, O1s, N1s and Ag3d, centered at 285, 533, 400 and 386.3 eV, respectively. For the paper sample, additional minor peaks are Al2p (74 eV), Si2p (102 eV), Ca2p (347 eV). These elements come from the industrial formulation of the paper samples purchased at a local store. PPy exhibits other features: S2p (168 eV) from the dopant as well as Fe2p doublet (~ 712–725 eV) arising from the oxidizing agent.

N1s is relatively more intense after in situ deposition of PPy (Fig. 2, PPy/Pap) whereas a prominent Ag3d doublet is noticed after the in-situ deposition of zero valent silver nanoparticles on top of the PPy/Pap substrate. The high resolution Ag3d doublet is shown in inset of Fig. 2 indicates indeed a binding energy position of 368.3 eV for the $Ag3d_{5/2}$ peak, in line with zero valent metal nanoparticles.

The C/N ratio was found to decrease in the order paper (82.4) > PPy/Pap (17.9) ~ AgNPs-PPy/Pap (18.2). This trend parallels the observation of black polypyrrole with the naked eye. It also indicates that the PPy/Pap substrate retains its C/N ratio after in situ silver deposition. Note, however, that the C/N exceeds the theoretical value of 4 for bulk polypyrrole and ~ 5 for the surface composition of polypyrrole (Beamson et al 1993). This indicates that the paper substrate is detected through the continuous PPy coating.

Figure 3 compares the narrow C1s regions from paper, PPy/Pap (1h) and AgNPs-PPy/Pap samples. Interestingly, the C1s region of the pristine paper sample is characteristic of a cellulosic substrate in that it has a prominent C-O component at ~ 286.7 eV and a second component at 288 eV due to acetal carbon type. The intense C-C/C-H C1s component is frequently observed on “real” cellulosic materials, industrially processed. The very last component at ~ 289 eV is due to carboxylic type carbon atoms, also noted by Beamson and Briggs (Omastová et al 2005).

For AgNPs-PPy/Pap sample, the fine structure of the C1s region is drastically changed: the peak is broad, and tailing. It also exhibits a subtle increase in the baseline at high binding energy side, which markedly differs from the rather flat background of the paper C1s peak in the case of the paper substrate. This step

below the peak maximum is actually invariably noticed in the case of polypyrrole surfaces (Boukerma et al 2007).

Interestingly, the C1s narrow region from PPy(1h)/Pap sample has a shape that resembles that of the underlying paper, with a narrow C-C/C-H component, together with an intense C-O C1s component at ~ 286.5 eV. Although slight peak broadening can be noticed, obviously the 1h deposition time is not sufficient to have a polypyrrole coating with a C1s feature that is shaped like that of pure polypyrrole. This is one reason why in this work, we have spent time and effort tuning the deposition conditions for polypyrrole and Ag. Interestingly, despite a high C/N atomic ratio, the C1s narrow region heavily reflects the C1s shape for pure polypyrrole and that the shape observed for the cellulosic paper starts to be screened by that of polypyrrole.

Nitrogen is a unique elemental marker for polypyrrole, and it is worth to inspect its N1s in comparison to that detected at the paper surface. Figure 4a shows a quasi-symmetrical, noisy peak for pristine paper at 400.0 eV. The polypyrrole exhibits a complex shape fitted with four components centered at 398.0, 399.7, 401.1 and 402.5eV, assigned to C = N defects (6.7 %), N-H, and two positively charged nitrogen atoms noted N_I^+ and N_{II}^+ the contribution of which is 23.1 %, in line with true conductive polypyrrole specimen (Fig. 4b). The situation is similar for AgNPs-PPy/Pap, the positively charged nitrogen atoms of which contribute 23.8% (Fig. 4c). This demonstrates that polypyrrole coating serves as support for the in-situ deposition of silver without any significant change in its chemical structure. Interestingly, one can note an even smaller C = N contribution to the total N1s peak (3.4%), and an additional peak at 406.4 eV assigned to nitrate from $AgNO_3$ precursor.

Scanning Electron Microscope coupled with energy dispersive X-ray spectrometry and X-ray diffraction spectroscopy of AgNPs-PPy composite films

Figure 5 (a) and (b) are the SEM micrographs of the PPy and AgNPs-PPy films, respectively. (c) EDX spectrum of the AgNPs-PPy film. (d) XRD patterns of the pristine PPy and AgNPs-PPy film.

The X-ray diffractograms of the PPy film before and after deposition of AgNPs confirmed the combination of AgNPs in the PPy matrix as shown in Fig. 5d. We can observe several peaks, indicating that the sample is crystallized. The broad peak centered at 2θ = 22.4° is due to the amorphous phase of PPy (ˇSkodovà et al 2013). The peaks located at 2θ values of 37.92°, 44.37°, 64.49° and 81.44° are matched well with the (111), (200), (220) and (222) crystal planes of the face-centered cubic Ag phase, respectively. The mean size of the crystallites, by using Scherrer’s formula for the face-centered cubic plane (111), was estimated to be of 3.7 nm. From the XRD patterns, existence of AgNPs in PPy matrix was established, which is consistent with the result of the SEM.

Electrochemical Activity Of Ppy/pap And Agnps-ppy/pap Materials

Electrochemical activity of PPy/Pap film obtained at different synthesizing durations and AgNPs-PPy/Pap electrode was investigated by cyclic voltammetry in the solution of 0.1 mol.l^{-1} KOH, as shown in Fig. 6. Oxidation and reduction processes were not observed in the voltammograms and a resistive response was obtained. Repeated scans show no significant changes in the voltammograms characteristics; this is probably due to several reasons such as low conductivity of the films, pH of the medium and the high sweeping rate. This behavior was observed in the case of PPy deposits on polyester textiles (Molina et al 2008; Molina et al 2009). The current density is slightly enhanced on PPy film synthesized during 2h (Fig. 5b) and the voltammogram of the AgNPs-PPy film had higher slope (less resistance) than that for the sample of PPy, indicating that the conductive properties of the PPy composites increased with the loading of Ag nanoparticles (Lu et al 2012; Tian et al 2017].

Indeed, electrochemical impedance spectroscopy is a well-established and powerful tool in the study of electrochemical behavior of materials, in particular, the estimation of the charge-transfer resistance (Rt) which is in relation with the reactivity of the studied materials (PPy/Pap and AgNPs-PPy/Pap). Figure 7 shows the Nyquist plots of the synthesized electrodes at the equilibrium open circuit potential (-350 mV versus SCE) and in 0.1M of potassium hydroxide solution. The experiments were carried out at the frequency range of 100 kHz to 100 mHz.

The semicircle feature and the EIS line indicate that the electrode process is controlled by electrochemical reaction at high frequencies and by mass transfer at low frequencies (Sen et al 2013). The semicircle is associated with the charge transfer (Rt) occurring at the electrode/electrolyte interface and double layer capacitance. By using Setup ZSimDemo 320 program, the impedance diagrams can be fitted by a simple equivalent circuit (insert of Fig. 8) composed by Rs (solution resistance), Rt (charge transfer resistance), w (Warburg contribution) and CPE (constant phase element of double layer capacitance (Cdl)). The charge-transfer resistance (Rt) values used in equation were given by the Setup_ZSimDemo_320 program by fitting the Nyquist plots.

The results indicate that the value of Rt is low (115 ohm.cm^{-2}) when the PPy film is deposited on sheet during 2 h compared to those deposited during 1 h (169 Ω.cm^{-2}) and 3h (260 Ω.cm^{-2}). The lowest value of Rt (98 Ω) is found when the PPy is decorated by Ag nanoparticles deposited during 10 min on PPy. The lower charge-transfer resistance (Rt) is indicative of the improvement conductivity (Benchikh et al 2009). For the unmodified PPy electrodes, the impedance curves register a large Warburg region indicates great variation in the ion diffusion path length and an increase in ion movement obstruction in the process of ion diffusion into the interior of the electrodes. Evidently, Ag dopant in PPy promotes the ion diffusion rate and is beneficial for a fast-current response in electrochemical reactivity (Yuana et al 2016). This result was consistent with the improved reactivity responses shown in cyclic voltammograms (Fig. 6). So, the value of 2h as synthesis time was chosen as the optimum value which gave the best results in relation with PPy reactivity and the best reactivity and conductivity are obtained when PPy film is modified by silver nanoparticles deposited during 10 min.

Conclusion

In this work we have fabricated new AgNPs-PPy composites onto paper substrate in two steps: (i) in situ deposition of polypyrrole, followed by (ii) in situ reduction of silver nitrates on PPy-coated paper. The polypyrrole deposition was optimized in order to obtain the highest electrochemical redox behavior of polypyrrole. The optimized polypyrrole coating served then for the in situ depsotion of zero valent Ag nanoparticles. From the above, we provide low cost, simple and environmentally friendly processes for the transformation of a non-conductive cellulosic paper into a multicomponent layered material, namely AgNPs-PPy/Pap. Last but not least, the composite paper electrodes described in this work can withstand any electrochemical reaction in alkaline media where other standard electrodes get readily corroded. The process presented here is scalable and the paper electrodes can be simply cut with scissors at the desired size and shape.

Declarations

Acknowledgements

Authors wish to acknowledge the Algerian Ministry of Higher Education and Scientific Research for supporting this work.

References

1. Hamam A, Oukil D, Dib A, Hammache H, Makhloufi L and Saidani B (2015) Polypyrrole coated cellulosic substrate modified by copper oxide as electrode for nitrate electroreduction, Surf. Rev. Lett. 22 : 1550065. https://doi.org/10.1142/S0218625X15500651
2. Aitout R, Belgaid A, Makhloufi L, Saidani B (2006) Synthesis of conducting poly-ortho-methoxy-aniline films onto an inert support (Plexiglas) and their modification with gold by cementation: electrocatalytique tests versus oxidation of hydrazine and proton reduction, React. Funct. Polym. 66 : 373-377. https://doi.org/10.1016/j.reactfunctpolym.2005.08.010
3. Santhiago M, Bettini J, Araújo S.R and C Bufon (2016) Three-Dimensional Organic Conductive Networks Embedded in Paper for Flexible and Foldable Devices, ACS Appl. Mater. Interfaces. 8 : 10661−10664. https://doi.org/10.1021/acsami.6b02589
4. Tian J, Peng D, Wu X, Li W, Deng H, Liu S (2017) Electrodeposition of Ag nanoparticles on conductive polyaniline/cellulose aerogels with increased synergistic effect for energy storage, Carbohydr. Polym. 156 : 19–25. https://doi.org/10.1016/j.carbpol.2016.09.005
5. Jia H, Wang J, Zhang X and Wang Y (2014) Pen-Writing Polypyrrole Arrays on Paper for Versatile Cheap Sensors, ACS Macro Lett. 3 : 86−90. https://doi.org/10.1021/mz400523x
6. Ma P, Zhu H, Wei J, Zhang M (2015) Facile fabrication of Au nanoparticles immobilized on polyaniline nanofibers: high sensitive nonenzymatic hydrogen peroxide sensor, Nanosci. Nanotechnol. Lett. 7 : 127–133. https://doi.org/10.1166/nnl.2015.1906

7. Kazemi S.H, Hosseinzadeh B, Zakavi S (2015) Electrochemical fabrication of conducting polymer of Ni-porphyrin as nano-structured electrocatalyst for hydrazine oxidation, Sens. Actuators B: Chem.210 : 343-348. https://doi.org/10.1016/j.snb.2014.12.131
8. ˇSkodovà J, Kopecky D, Vrnata M, Varga M, Prokes J, Cieslar M, Bober P and Stejskal J, (2013) Polypyrrole–silver composites prepared by the reduction of silver ions with polypyrrole nanotubes, Polym. Chem. 4 : 3610-3616. https://doi.org/10.1039/C3PY00250K
9. Hara S, Zama T, Ametani A, Takashima W, Kaneto K (2004) Enhancement in electrochemical strain of a polypyrrole–metal composite film actuator, J. Mater. Chem.14 : 2724-2725. https://doi.org/10.1039/B409169H
10. Liu Y.C, Yang K.H (2006) Catalytic electroxidation pathway for electropolymerization of polypyrrole in solutions containing gold nanoparticles, Electrochim. Acta. 51 : 5376-5382. https://doi.org/10.1016/j.electacta.2006.02.013
11. Oukil D, Benhaddad L, Makhloufi L, Aitout R and Saidani B (2013) Gold nanoparticles modified Polypyrrole/Iron electrode used as sensor for hydrazine detection, Sens. Lett. 11 : 395-404. https://doi.org/10.1166/sl.2013.2731
12. Mokrane S, Makhloufi L, and Alonso-Vante N (2008) Electrochemistry of platinum nanoparticles supported in polypyrrole (PPy)/C composite materials, J Solid State Electrochem.12 : 569-574. https://doi.org/10.1007/s10008-007-0398-x
13. You C, Han C, Wang X, Zheng Y, Li Q, Hu X, Sun H (2012) The progress of silver nanoparticles in the antibacterial mechanism, clinical application and cytotoxicity, Mol. Biol. Rep. 39 : 9193-9201. https://doi.org/10.1007/s11033-012-1792-8
14. Maráková N, Humpolí ˇcek P, Ka ˇspárková V, Capáková Z, Martinková L, Bober P, Trchová M, Stejskal J (2017) Antimicrobial activity and cytotoxicity of cotton fabric coated with conducting polymers, polyaniline or polypyrrole, and with deposited silver nanoparticles, Appl. Surf. Sci. 396 : 169–176. https://doi.org/10.1016/j.apsusc.2016.11.024
15. Lu Y, Chen W (2012) Sub-nanometre sized metal clusters: from synthetic challenges to the unique property discoveries, Chem. Soc. Rev. 41 : 3594-3623. https://doi.org/10.1039/C2CS15325D
16. Nia P.M, Meng W.P, Alias Y (2015) Hydrogen peroxide sensor: Uniformly decorated silver nanoparticleson polypyrrole for wide detection range, Appl. Surf. Sci. 357 : 1565–1572. https://doi.org/10.1016/j.apsusc.2015.10.026
17. Bonacic-Koutecky V, Kulesza A, Gell L, Mitric R, Antoine R, Bertorelle F, Ramouda R, Rayane D, Broyer M, Tabarin T, Dugourd P (2012) Silver cluster–biomolecule hybrids: from basics towards sensors, Phys. Chem. Chem. Phys. 14 : 9282-9290. https://doi.org/10.1039/C2CP00050D
18. Sparavigna A. C, Florio L, Avloni J, Henn A (2010) Polypyrrole Coated PET Fabrics for thermal applications, Mater. Sci. Appl. 1 : 253-259. https://doi:10.4236/msa.2010.14037
19. Sain M, Panthapulakkal S (2006) Bioprocess preparation of wheat straw fibers and their characterization, Ind. Crop. Prod. 23 : 1–8. https://doi.org/10.1016/j.indcrop.2005.01.006

20. Kaushik A, Singh M (2011) Isolation and characterization of cellulose nanofibrils from wheat straw using steam explosion coupled with high shear homogenization, Carbohydr. Res. 346 : 76–85. https://doi.org/10.1016/j.carres.2010.10.020
21. He Q, Huang Z, Liu Y (2007) Template-directed one-step synthesis of flowerlike porous carbonated hydroxyapatite spheres, Mater. Lett. 61 :141–143. https://doi.org/10.1016/j.matlet.2006.04.082
22. Hu W, Chen S, Yang Z, Liu L (2011) Flexible Electrically Conductive Nanocomposite Membrane Based on Bacterial Cellulose and Polyaniline. L Phys. Chem. B. 115 : 8453-8457. https://doi.org/10.1021/jp204422v
23. Ul-Islama M, Khana T, Kon-Parka J (2012) Nanorein forced bacterial cellulose–montmorillonite composites for biomedical applications, Carbohydr. Polym. 89 : 1189–1197. https://doi.org/10.1016/j.carbpol.2012.03.093
24. Yuana L, Wan C, Yeb X, Wua F (2016) Facial Synthesis of Silver-incorporated Conductive Polypyrrole Submicron Spheres for supercapacitors, Electrochimica Acta. 213 : 115–123. https://doi.org/10.1016/j.electacta.2016.06.165
25. Feng X.M, Huang H.P, Ye Q.Q, Zhu J.J, Hou W.H (2007) Ag/Polypyrrole core-Shell nanostructures: interface polymerization, characterization, and modification by gold nanoparticles, J. Phys. Chem. 111 :8463-8468. https://doi.org/10.1021/jp071140z
26. Wei Y.Y, Li L, Yang X.M, Pan G.L, Yan G.P, Yu X.H (2010) One-step UV-induced synthesis of polypyrrole/Ag nanocomposites at the water/ionic liquid interface, Nanoscale Res. Lett. 5 : 433-437. https://doi.org/10.1007/s11671-009-9501-9
27. Patil D.S, Pawar S.A, Devan R.S, Gil Gang M, Ma Y.R, Kim J.H, Patil P.S (2013) Electrochemical supercapacitor electrode material based on polyacrylic acid/polypyrrole/silver composite, Electrochim. Acta. 105 : 569-577. https://doi.org/10.1016/j.electacta.2013.05.022
28. Das D, Nath B.C, Phukon P, Saikia B.J, Kamrupi I.R, Dolui S.K (2013) Nickel oxide/polypyrrole/silver nanocomposites with core/shell/shell structure: Synthesis, characterization and their electrochemical behaviour with antimicrobial activities, Mater. Chem. Phys. 142 : 61-69. https://doi.org/10.1016/j.matchemphys.2013.06.040
29. Wang J, Neoh K.G, Kang E.T (2004) Comparative study of chemically synthesized and plasma polymerized pyrrole and thiophene, Thin solid films. 446 : 205–217. https://doi.org/10.1016/j.tsf.2003.09.074
30. Zhang C.X., Li C, Chen Y.Y, Zhang Y (2014) Synthesis and catalysis of Ag nanoparticles trapped into temperature-sensitive and conductive polymers, J. Mater. Sci. 49 : 6872-6882. https://doi.org/10.1007/s10853-014-8389-7
31. Beamson G and Briggs D (1993) High-resolution XPS of Organic Polymers: The Scienta ESCA300 Database, John Wiley & Sons, Chichester. 5: 778-778. https://doi.org/10.1002/adma.19930051035
32. Omastová M, Boukerma K, Chehimi M.M, Trchova M (2005) Novel silicon carbide/polypyrrole composites; preparation and physicochemical properties, Mater. Res. Bull. 40 : 749-765. https://doi.org/10.1016/j.materresbull.2005.02.010

33. Boukerma K, Micu˘s˘ık M, Mravc˘akov M, Omastov M, Vaulay M.J, Beaunier P, Chehimi M. M (2007) Surfactant-assisted control of the surface energy and interfacial molecular interactions of polypyrrole. Colloids and Surfaces A: Physicochem. Eng. Aspects. 293 : 28–38. https://doi.org/10.1016/j.colsurfa.2006.07.005

34. Molina J, del Río A.I, Bonastre J, Cases F (2008) Chemical and electrochemical polymerisation of pyrrole on polyestertextiles in presence of phosphotungstic acid, Eur. Polym. J. 44 : 2087–2098. https://doi.org/10.1016/j.eurpolymj.2008.04.007

35. Molina J, del Rio A.I, Bonastre J, Cases F (2009) Electrochemical polymerisation of aniline on conducting textilesof polyester covered with polypyrrole/AQSA, Eur. Polym. J. 45 :1302–1315. https://doi.org/10.1016/j.eurpolymj.2008.11.003

36. Tian J, Peng D, Wu X, Li W, Deng H, Liu S (2017) Electrodeposition of Ag nanoparticles on conductive polyaniline/cellulose aerogels with increased synergistic effect for energy storage, Carbohydr. Polym. 156 : 19–25. https://doi.org/10.1016/j.carbpol.2016.09.005

37. Sen P, De A, Chowdhury A.D, Bandyopadhyay S.K, Agnihotri N, Mukherjee M (2013) Conducting polymer-based manganese dioxide nanocomposite as supercapacitor, Electrochim. Acta, 108 : 265-273. https://doi.org/10.1016/j.electacta.2013.07.013

38. Benchikh A, Aitout R, Makhloufi L, Benhaddad L, Saidani B (2009) Soluble conducting poly(aniline-co-orthotoluidine) copolymer as corrosion for carbon steel in 3% NaCl solution, Desalination. 249 : 466-474. https://doi.org/10.1016/j.desal.2008.10.024

Figures

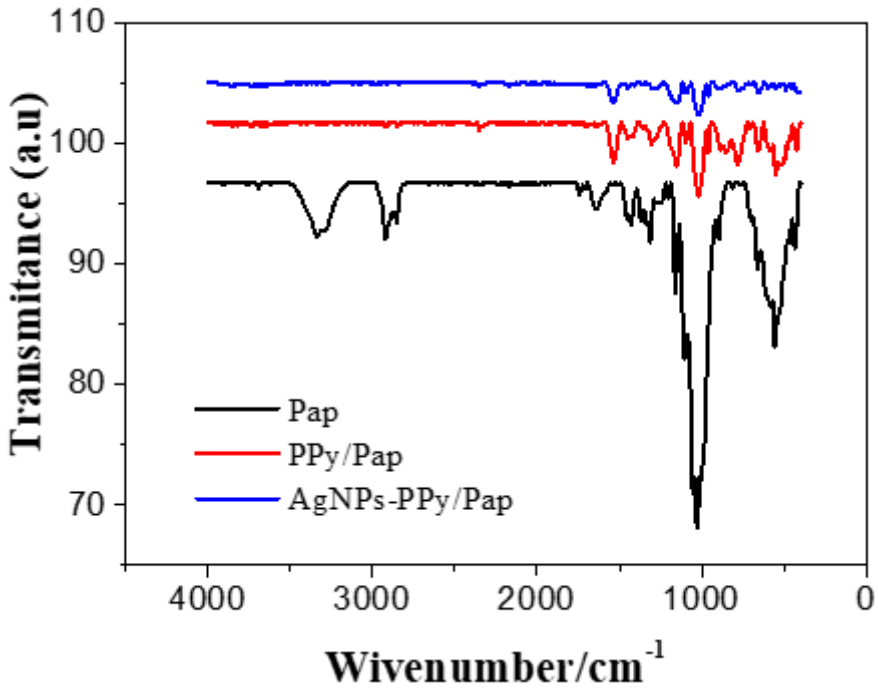

Figure 1

FTIR spectra of: Cellulosic paper (Pap), PPy/Pap (2h) and AgNPs-PPy/Pap. The AgNPs-PPy/Pap preparation conditions: 2h polymerization; 2mM AgNO3 reduced for 10 min.

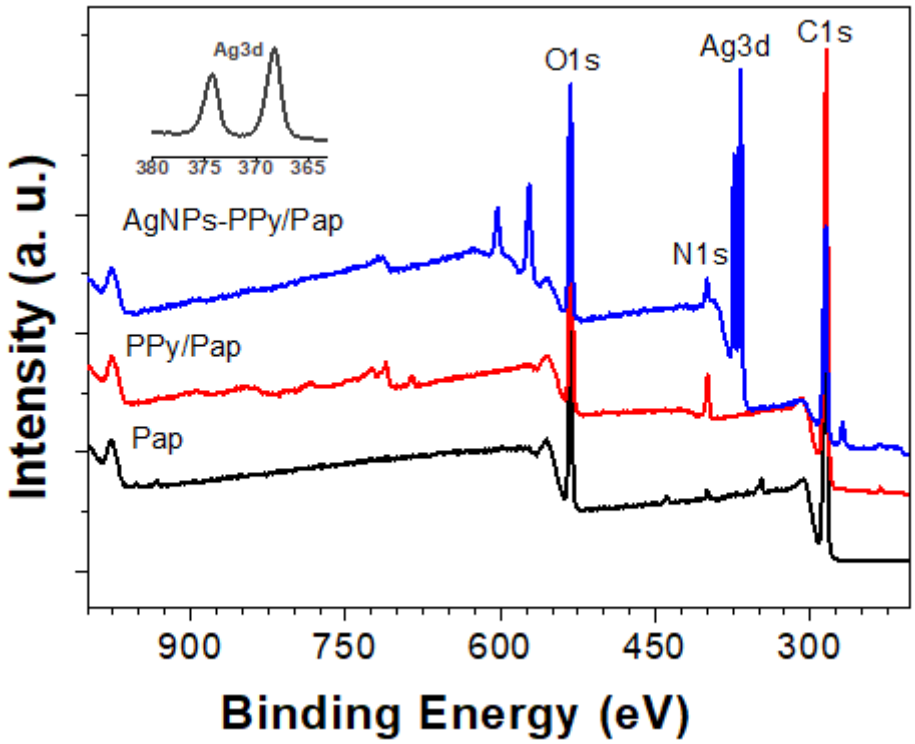

Figure 2

XPS survey spectra of pristine paper, PPy/Pap (2h) and AgNPs-PPy/Pap samples. Ag3d is shown in inset for AgNPs-PPy/Pap. The AgNPs-PPy/Pap preparation conditions: 2h polymerization; 2mM AgNO3 reduced for 10 min.

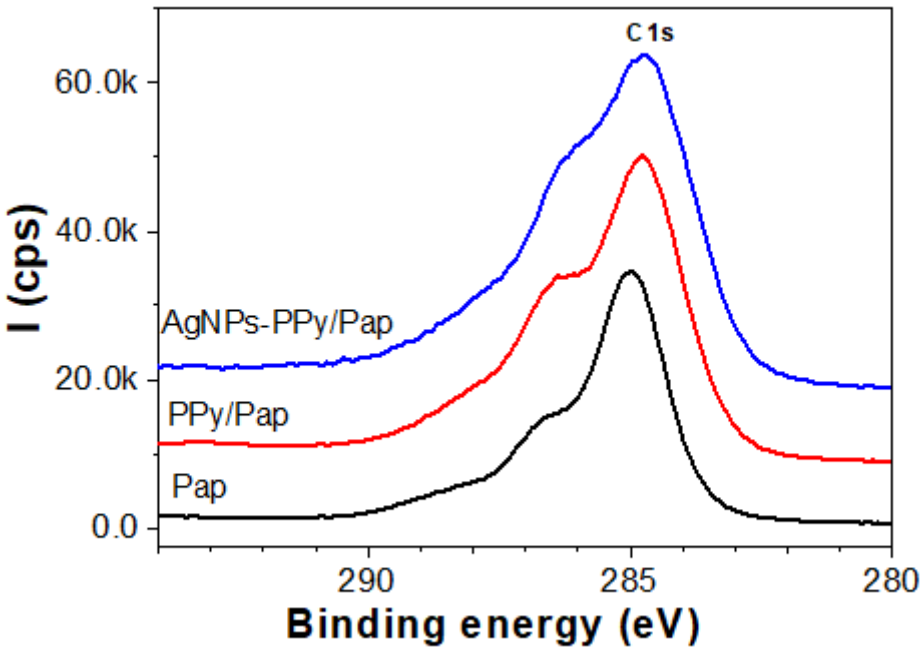

Figure 3

C1s narrow regions of pristine paper, PPy/Pap (1h), and AgNPs-PPy/Pap samples. The AgNPs-PPy/Pap preparation conditions: 2h polymerization; 2mM AgNO3 reduced for 10 min.

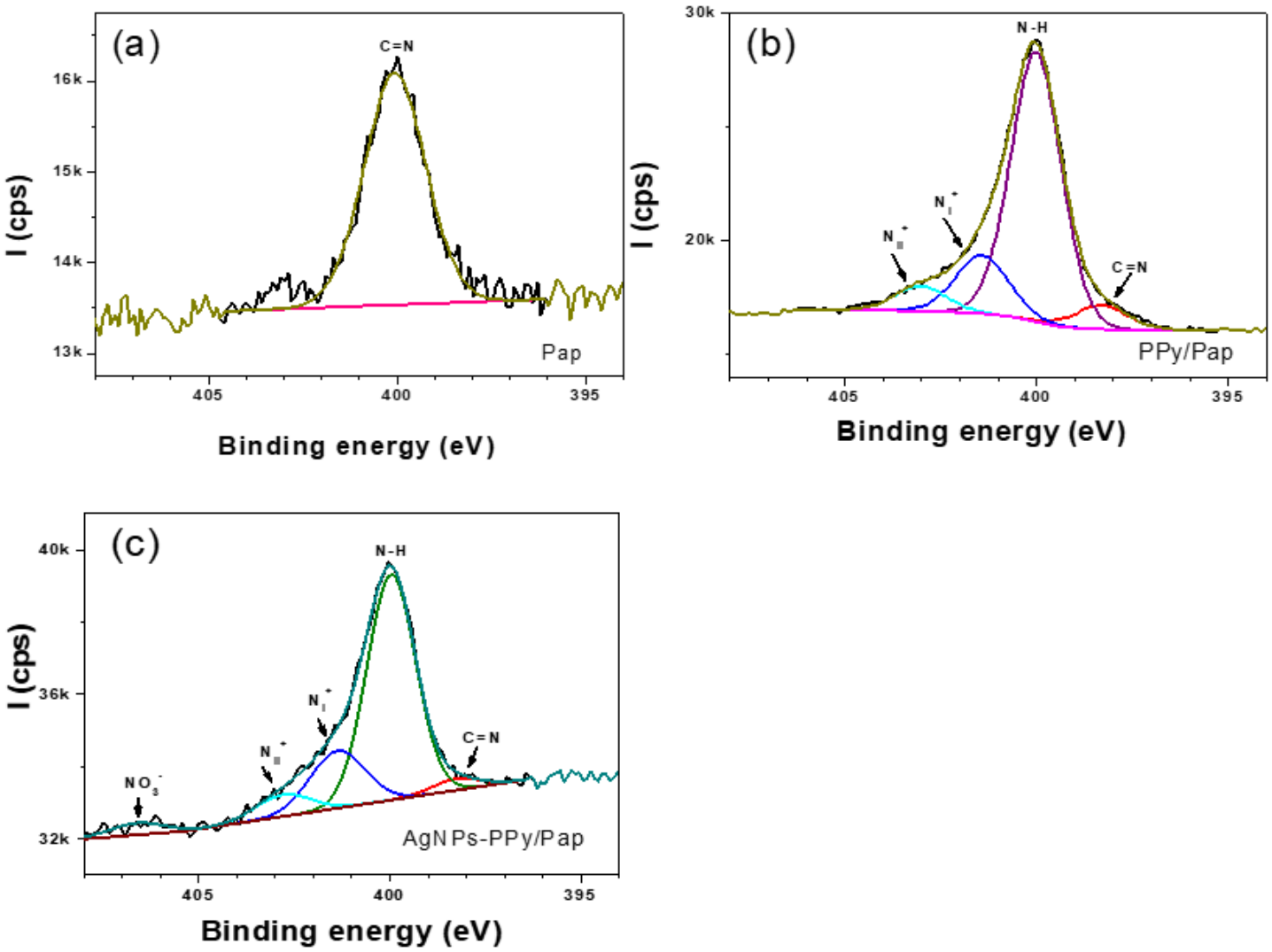

Figure 4

XPS survey spectra of pristine (a) Pap, (b) PPy/Pap (2h) and (c) AgNPs-PPy/Pap samples. The AgNPs-PPy/Pap preparation conditions: 2h polymerization; 2mM AgNO3 reduced for 10 min.

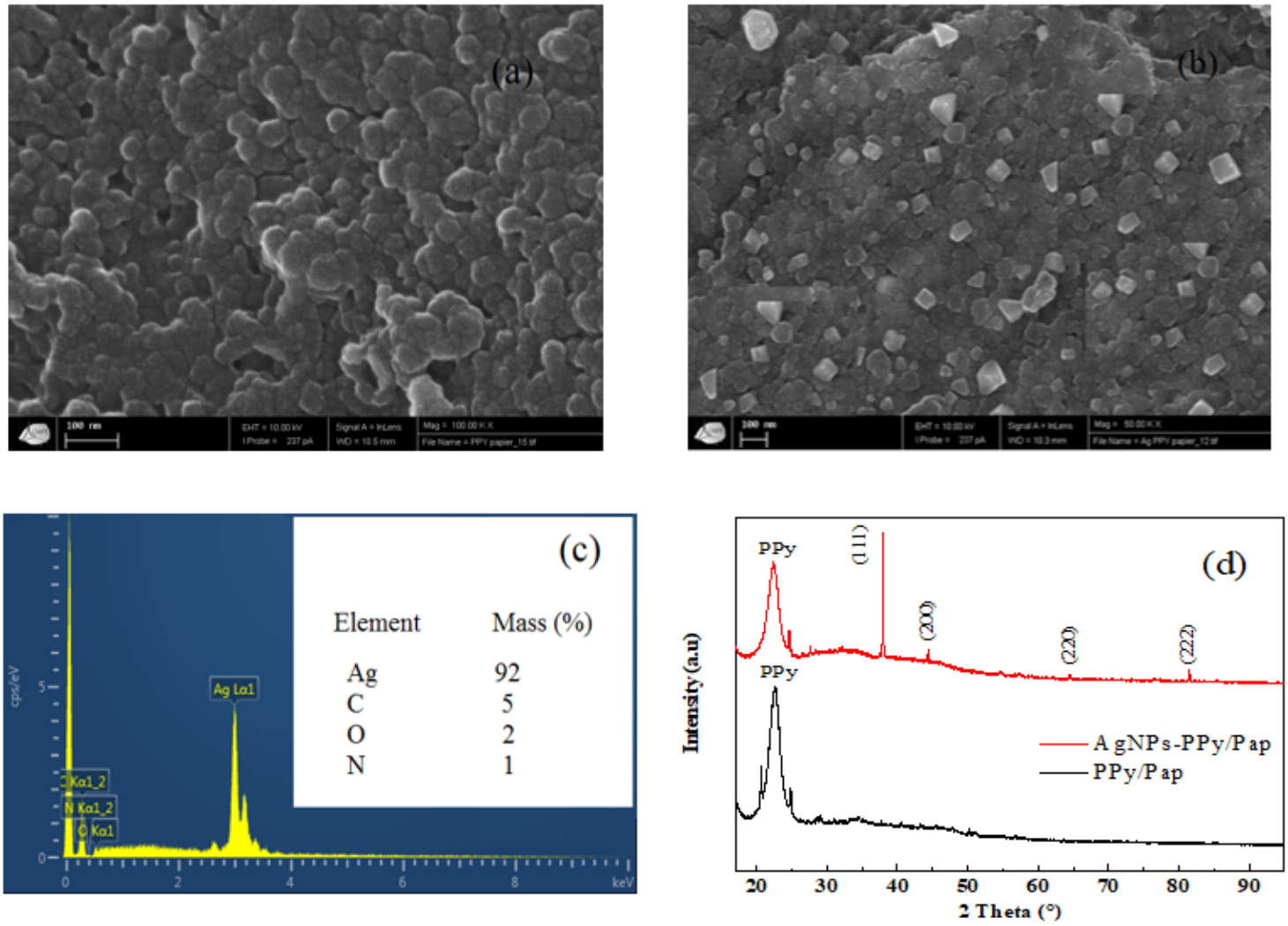

Figure 5

(a) and (b) are the SEM micrographs of the PPy and AgNPs-PPy films, respectively. (c) EDX spectrum of the AgNPs-PPy film. (d) XRD patterns of the pristine PPy and AgNPs-PPy film.

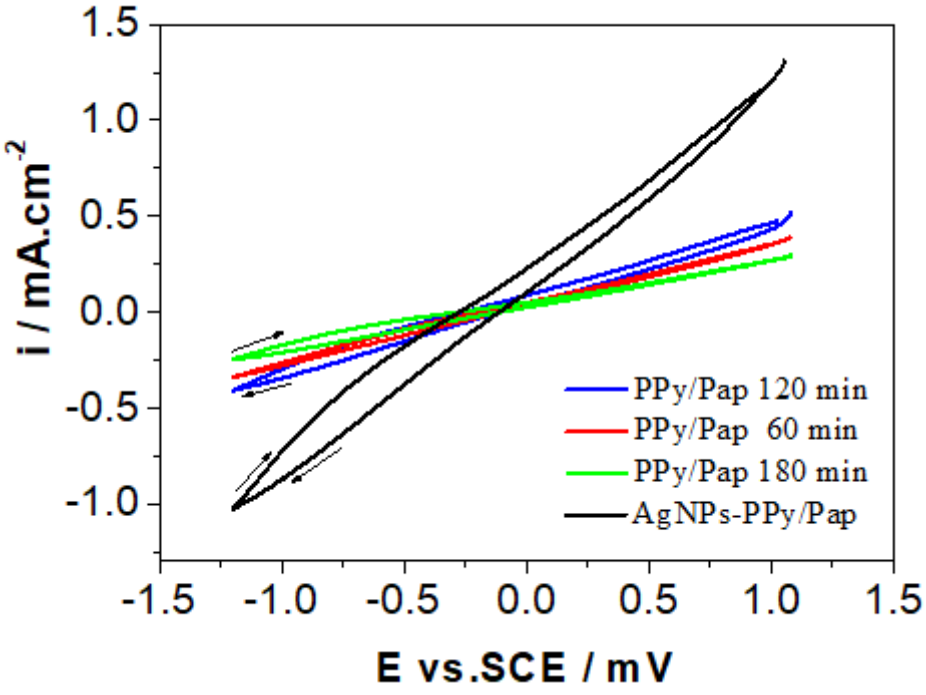

Figure 6

Cyclic voltammograms of the PPy/Pap electrodes obtained with different synthesis durations and AgNPs-PPy/Pap electrode. (PPy synthesis conditions: oxidant Iron (III) chloride 0.2 M, concentration of pyrrole 0.1M and T= 0°C). (Ag deposited onto PPy/Pap (2h) while 10 min and 2 mM AgNO3) in 0.1 M of KOH. Scan rate of 20mVs-1. All electrodes have 2 cm2 geometric surfaces.

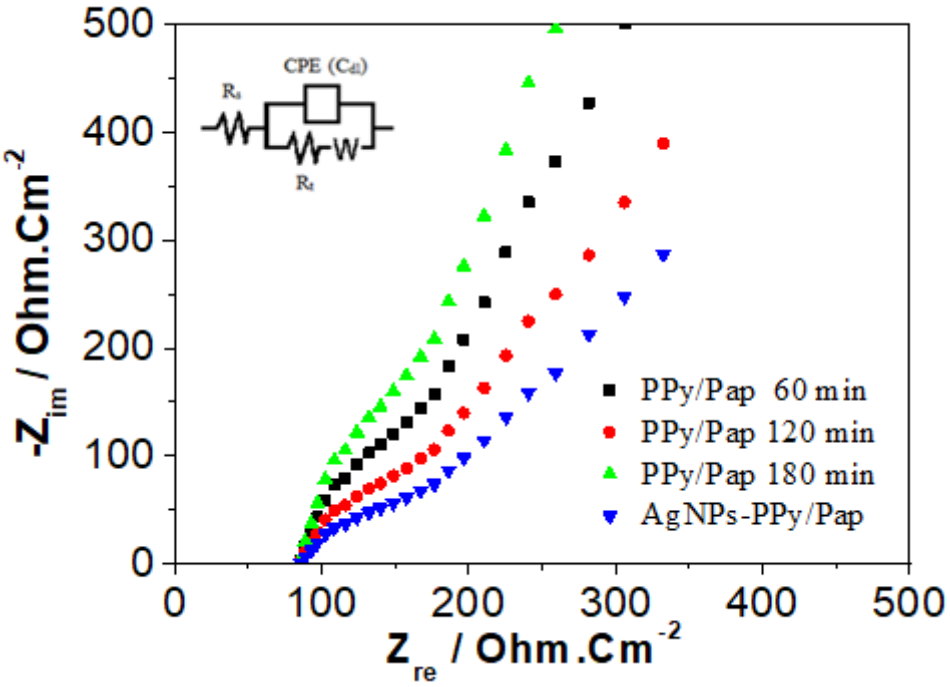

Figure 7

Nyquist diagrams of the PPy/Pap (obtained with different synthesis durations) and AgNPs-PPy/Pap electrodes at the equilibrium open circuit potential of - 350 mVvs. SCE and in 0.1 M of KOH. PPy synthesis conditions: $FeCl_3$ 0.2 M, concentration of pyrrole 0.1M and T= 0°C. Ag deposited onto PPy/Pap (2h) while 10 min and 2 mM $AgNO_3$.